J. Cell. Mol. Med. Vol 12, No 1, 2008 pp. 174-186

In vivo detection of c-Met expression in a rat C6 glioma model

R. A. Towner [a, c, *], N. Smith [a], S. Doblas [a, e], Y. Tesiram [a], P. Garteiser [a], D. Saunders [a], R. Cranford [a], R. Silasi-Mansat [b], O. Herlea [b], L. Ivanciu [b], D. Wu [d], F. Lupu [b]

[a] *Small Animal MRI Core Facility, Oklahoma City, OK, USA*
[b] *Cardiovascular Biology Research Programs, Oklahoma Medical Research Foundation, Oklahoma City, OK, USA*
[c] *Department of Pathology, The University of Oklahoma Health Sciences Center, Oklahoma City, OK, USA*
[d] *Department of Radiological Sciences, The University of Oklahoma Health Sciences Center, Oklahoma City, OK, USA*
[e] *Oklahoma University Bioengineering Center, Norman, Oklahoma, OK, USA*

Received: November 19, 2007; Accepted: December 19, 2007

Abstract

The tyrosine kinase receptor, c-Met, and its substrate, the hepatocyte growth factor (HGF), are implicated in the malignant progression of glioblastomas. *In vivo* detection of c-Met expression may be helpful in the diagnosis of malignant tumours. The C6 rat glioma model is a widely used intracranial brain tumour model used to study gliomas experimentally. We used a magnetic resonance imaging (MRI) molecular targeting agent to specifically tag the cell surface receptor, c-Met, with an anti-c-Met antibody (Ab) linked to biotinylated Gd (gadolinium)-DTPA (diethylene triamine penta acetic acid)-albumin in rat gliomas to detect overexpression of this antigen *in vivo*. The anti-c-Met probe (anti-c-Met-Gd-DTPA-albumin) was administered intravenously, and as determined by an increase in MRI signal intensity and a corresponding decrease in regional T_1 relaxation values, this probe was found to detect increased expression of c-Met protein levels in C6 gliomas. In addition, specificity for the binding of the anti-c-Met contrast agent was determined by using fluorescence microscopic imaging of the biotinylated portion of the targeting agent within neoplastic and 'normal' brain tissues following *in vivo* administration of the anti-c-Met probe. Controls with no Ab or with a normal rat IgG attached to the contrast agent component indicated no non-specific binding to glioma tissue. This is the first successful visualization of *in vivo* overexpression of c-Met in gliomas.

Keywords: molecular-targeted MRI • c-Met • gliomas • biotinylated-anti-c-Met-Gd-DTPA-albumin • rat, *in vivo*

Introduction

Gliomas are classified by the World Health Organization according to their morphologic characteristics into astrocytic, oligodendroglial and mixed tumours [1]. Gliomas comprise the majority of primary brain tumours diagnosed [2, 3]. Due to the infiltrative and invasive nature of gliomas, surgery is rarely effective, that is after surgical removal tumours recur predominantly within 1 cm of the resection cavity [4, 5]. Despite modern diagnostics and treatments the median survival time for patients with aggressive gliomas, glioblastoma multiforme, does not exceed 15 months [5, 6].

Numerous intracranial rat brain tumour models have been used to study gliomas, including some

*Correspondence to: Rheal A. TOWNER, Ph.D.,
Director, Small Animal MRI Core Facility,
Associate Member and Director,
Free Radical Biology & Aging Research Program,
825 NE 13th St., Oklahoma City,
OK 73104, USA.
Tel.: +(405) 271-7383; Fax: +(405)-271-7254
E-mail: Rheal-Towner@omrf.org

doi: 10.1111/j.1582-4934.2008.00220.x

that are aggressive. The C6 intracerebral rat model for gliomas is well accepted for experimental studies and has been extensively used by numerous investigators [7–9]. C6 glioma tumours in rats have been previously shown to have significant degrees of invasion characterized by a diffuse infiltrating border where individual cells invade the surrounding brain tissue, and that these characteristics closely resemble natural gliomas [8, 10, 11]. The C6 glioma model resembles a medium (grade II) to high-grade glioma (grade IV, glioblastoma multiforme) in humans [12, 13].

The poor prognosis associated with high-grade gliomas in humans may perhaps improve if earlier and more accurate diagnoses can be made. A tumour marker of interest is the tyrosine kinase receptor, c-Met, for the hepatocyte growth factor (HGF). The c-Met proto-oncogene encodes a 190 kD transmembrane tyrosine kinase glycoprotein composed of a transmembrane β-subunit of145 kD, with both extracellular and intracellular components, and a 50 kD extracellular α-subunit [14]. The latter was identified as the receptor for a polypeptide known as HGF found on several cell types mainly of epithelial origin. c-Met is crucially involved in invasive cell growth and motility during embryogenesis, and has been detected in many invasive tumours, including gliomas, meningiomas, colorectal cancer, uveal melanomas, thyroid carcinomas, breast carcinomas, gastric carcinomas, hepatocarcinomas and sarcomas [15–19]. Expression of HGF has been shown to be associated with poor prognosis of malignant gliomas, and HGF has also been used as a predictor for recurrence of meningiomas [20]. Both HGF and c-Met have emerged as key determinants of brain tumour growth and angiogenesis [21, 22].

With the use of magnetic resonance imaging (MRI) morphological and functional processes can be studied *in vivo* and non-invasively, allowing serial studies in experimental animals and humans to be conducted. In human glioblastomas, MRI typically reveals a central 'ring-enhancing mass', with contrast enhancement, emerging from within the infiltrative glioma and rapidly expanding outward [23]. The histopathologic features that can be used to distinguish glioblastoma from lower grade gliomas are mainly found near this contrast-enhancing rim, and these include foci of necrosis and microvascular hyperplasia, a form of angiogenesis [23].

MRI, whose images are constructed from the water content of the body, has considerably improved pathological diagnosis by detecting and localizing lesions to a certain extent, however molecular-specific information is often lacking. *In vivo* visualization of cell surface antigens and/or receptors can be done by using MRI molecular-targeted agents. This method relies on the specific labelling of extracellular cell surface receptors or antigens with a MRI-targeted contrast agent. The contrast agent MRI probe can be specifically targeted by a monoclonal antibody (mAb) which binds with high affinity to the receptor or antigen. Gadolinium (Gd)-based contrast agents have traditionally been used for non-specific contrast-enhanced clinical MRI. The Gd-based contrast agents provide a strong positive T_1 relaxation contrast. For instance, this approach has been successfully used to image with MRI the neovasculature in angiogenic tumours with Gd-labelled polymerized liposomes targeted against the $\alpha_V\beta_3$ integrin expressed on neovascular endothelium [24–26]. Konda *et al.* (2001) used a polyamidoamine (PAMAN) folate-dendrimer conjugated to folic acid and Gd-DTPA to specifically target the high-affinity folate receptor (hFR), which is overexpressed in more than 80% of ovarian tumours, *in vitro* in mouse erythroleukemia cells and *in vivo* in ovarian tumour xenografts, as another approach to amplify the amount of Gd reaching the tumour site [27]. A study by Artemov *et al.* (2003) used avidin-Gd-DTPA complexes targeted for tumour cells pre-labelled with a biotinylated anti-*Her-2/neu* mAb to obtain *in vivo* MR images of *Her-2/neu* expressing tumours in SCID mice [28].

In this study we used an intracerebral implantation C6 rat glioma model, to visualize for the first time increased *in vivo* expression of the c-Met antigen in neoplastic lesions with the use of a molecular-targeted compound with a MRI contrast agent, Gd-DTPA-albumin coupled to an Ab specific for c-Met.

Materials and methods

Intracranial rat brain tumour models

The heads of anaesthetized rats (male Fisher 344) were immobilized (stereotaxic unit; Stoelting, USA) and using an aseptic technique, a 1 mm burr hole was drilled in the skull 2 mm anterior and 2 mm lateral to the bregma on the right side. A 25 μl gas-tight Hamilton syringe was then used to stereotactically inject 10^4 rat C6 glioma cells (in 10 μl of

Dulbecco's-modified Eagle's medium supplemented with ultra-low temperature gelling agarose) into the right frontal lobe at a depth of 3 mm relative to the dural surface [29, 30]. C6 cell lines (ATCC) were maintained and expanded immediately prior to inoculation. Following injection, the skin was closed with a surgical suture [31, 32]. Rats were maintained on a choline-deficient (CD) diet, since the tumour cells used were previously found to be tumourigenic in CD Fisher rats [33]. MRI molecular targeting experiments were carried out 17–21 days after the initial injection of cells.

Syntheses of c-Met-specific MRI contrast agents

To recognize the c-Met antigen, a mouse monoclonal anti-c-Met Ab to the β-chain of c-Met (145 kD), which has an extracellular domain [34] (Met (B-2): sc-8057, Santa Cruz Biotechnology, Inc., CA, USA), was used. The contrast material, biotin-BSA (bovine serum albumin)-Gd-DTPA, was prepared by a modification of the method of Dafni *et al.* (2002) [35]. The biotin moiety was added to allow subsequent histological fluorescence localization. Biotin-BSA-GdDTPA was synthesized as follows: BSA (8 μmol; Sigma) was dissolved in 0.1 M sodium bicarbonate (pH 8.5). Sulfo-NHS-Biotin (53 μmol; Pierce) was dissolved in double distilled water and was added to BSA while stirring. The reaction mixture was stirred for 1 hr at 4°C and an additional 2 hrs at room temperature. The dialyzed product in 0.1 M Hepes buffer (pH 8.8) was reacted with diethylene triamine pentaacetic acid anhydride (DTPA, 1.4 mmol; Sigma) and suspended in dimethyl sulfoxide (DMSO) at room temperature. DTPA was added in small portions and the pH was adjusted immediately after each addition to 8.5 with 5 N NaOH. The reaction mixture was stirred for 2 hrs at 4°C and extensively dialyzed against cold 0.1 M citrate buffer (pH 6.5). Finally, gadolinium (III) chloride ($GdCl_3$, 0.67 mmol; Sigma) in 0.1 M sodium acetate buffer (pH 6.0) was added gradually and the mixture was stirred for 24 hrs at 4°C. The product, biotin-BSA-Gd-DTPA, was extensively dialyzed with cold citrate buffer (0.1 M, pH 6.5), then with double distilled water, and subsequently lyophilized. The contrast material biotin-BSA-Gd-DTPA was conjugated with the anti-c-Met Ab through a sulfo-NHS-EDC link between albumin and Ab according to protocol of Hermanson [36]. Briefly, to the solution of biotin-BSA-Gd-DTPA (9.7 mg/ml in double distilled water), a quantity of EDC (1-ethyl-3-[3-dimethylamino-propyl] carbodiimide hydrochloride), and sulfo-NHS were added to obtain final concentrations of 0.05 M EDC and 5 mM sulfo-NHS. The solution was mixed and reacted for 15 min. at room temperature. This activated solution was added directly to the solution of Ab (anti-cMet, 200 μg/ml) for conjugation. The mixture was left to react for at least 2 hrs at room temperature in the dark. The product was lyophilized and subsequently stored at 4°C and reconstituted to a desirable concentration in phosphate buffered saline (PBS) for injections [35]. The final amount of the product, anti-c-Met-biotin-BSA-Gd-DTPA that was injected (200 μl) into the rat (i.v. *via* tail vein) was estimated to be 200 μg anti-c-Met and 100 mg biotin-BSA-Gd-DTPA per injection. A normal rat IgG-biotin-BSA-Gd-DTPA agent was used as a control. This agent was used since it has a similar molecular weight to the anti-c-Met-biotin-BSA-Gd-DTPA agent, but is however non-immunogenic and non-specific for c-Met, that is should not specifically bind to tumour or normal tissues. The same procedure was followed (normal rat IgG obtained from a healthy rat population; cat. no. 20005-1; Apha Diagnostic International, San Antonio, TX, USA) for the preparation of this agent as was carried out for the anti-c-Met targeting agent.

MRI

MR equipment used was a Bruker Biospec 7.0 Tesla/30 cm horizontal-bore imaging spectrometer. MR experiments were carried out under general anaesthesia (1–2% Isoflurane and 0.8–1.0 L/min O_2). Images were obtained using a Bruker S116 gradient coil (maximum gradient strength 200 mT/m), in a cross-coil setup consisting of a rat head surface coil for RF (radio frequency) signal reception, and a 72 mm quadrature multi-rung coil for RF transmission. Anaesthetized restrained rats were placed in an MR probe, and their brains localized by MRI. Rats were then injected intravenously with c-Met antibodies tagged with the Gd-albumin-based anti-c-Met contrast agent (5 ml/kg; 1 mg Ab/kg; 0.4 mmol Gd^{3+}/kg) [24–26, 28]. Multiple ^{1}H-MR image slices were taken in the transverse plane using a multi-spin echo (SE) multi-slice (MS) sequence (MSME; repetition time (TR) 2.4 sec., echo times (TE) 17.4 (T_1-weighted) and 63.9 (T_2-weighted) ms, 128 x 128 matrix, four steps per acquisition, 3.5 x 3.5 cm^2 field of view, 1 mm slice thickness). The T_1-weighted images provided good anatomical detail of the rat brain, and the T_2-weighted images provided sufficient contrast for tumour location. For T_1 relaxation measurements, a variable TR spin-echo sequence (multiple TRs of 200, 400, 800, 1200 and 1600 ms) was used to obtain data before and after contrast agent injections for a period of 3 hrs. Other MR parameters were similar to those used for the MSME images. T_1 values were calculated from specific region-of-interests (ROIs) within normal brain and glioma regions. A decrease in T_1 relaxation and a corresponding increase in MR signal intensity indicated specific binding of Gd-based anti-c-Met probes in regions within the gliomas.

Following MRI experiments, rats were euthanized (gas CO_2 inhalation), and brains were immediately extracted and fixed for fluorescence staining.

Relative concentration maps for contrast agents

At all time points, the individual T_1 values of all pixels were estimated from their signal intensities $S(T_R)$ by a numerical non-linear fitting procedure against the following equation (1) [37]:

$$S(T_R) = S0.\ (1 - e^{-T_R/T_1}) \quad (1)$$

where T_R is the repetition time (units: ms), is the signal intensity (integer machine units) at $T_{R>>T1}$ and T_E=0 and T_1 is the longitudinal relaxation time constant (units: ms). The relative contrast agent concentrations C (units: M) were then computed for each pixel by assuming a proportional relation to differences in relaxation rates [37], as described in equation (2).

$$C \propto [1/T_1 - 1/T_1(C = 0)] \quad (2)$$

The values for T_1(C = 0) were taken from a measurement done prior to contrast agent injection. Relative concentration maps were then generated using a colour gradient from black (absence of contrast agent) to white (maximal concentration measured). All computation steps were performed using Mathematica 6.0 (Wolfram Research, Champaign, IL, USA).

Fluorescence staining

Indirect immunofluorescence staining of c-Met was done by incubating brain tissue cryosections with rabbit anti-c-Met antibodies followed by donkey anti-rabbit IgG-Cy3 in phosphate-buffered saline containing 0.1% v/v saponin. Brain tissue (glioma tissue and normal tissue in the contralateral side) was obtained following MRI investigations and *in vivo* intravenous administration of the molecular probes (anti-c-Met-, non-Ab- and normal rat IgG-biotin-BSA-Gd-DTPA agents) on the same animals. Staining for the biotinylated Gd-DTPA-albumin-anti-c-Met agent was done using a Cy3-labelled streptavidin to bind to the biotin functional group on the molecular-targeted agent. Stained tissue slices were viewed and photographed with a Nikon C1 confocal laser scanning microscope (Nikon Instruments, USA).

Western blots

Frozen tissue was weighed and sliced into thin pieces using a razor blade and then subsequently thawed in lysis buffer containing proteases and phosphatase inhibitors. Tissues were further disrupted and homogenized at 4°C, incubated on ice for 30 min., transferred to microcentrifuge tubes and centrifuged (10,000×*g*, 10 min., 4°C). The supernatant fluid was the total cell lysate. Several centrifugations were necessary to obtain a clear lysate. After determining the total protein concentrations, the lysates were separated on SDS-PAGE (Bio-Rad, Emeryville, CA, USA), and transferred to nitrocellulose membranes. Western analysis was done using antibodies against c-Met (as described above). Secondary antibodies were labelled

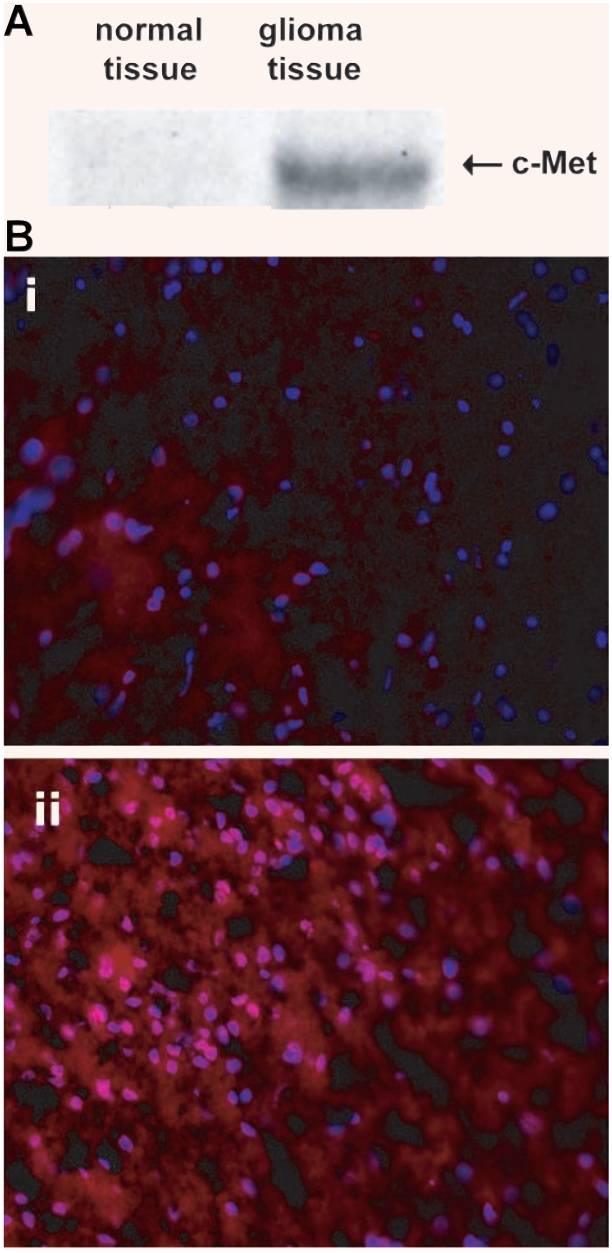

Fig. 1 (**A**) Western blot of c-Met in normal rat brain tissue, and a C6 glioma (18 days after implantation). (**B**) Immunofluorescence detection of c-MET (red florescence, 20x magnification) in (*i*) contralateral control brain tissue, and (*ii*) a glioma region in a C6-glioma-bearing rat (18 days after implantation of C6 cells). Nuclei are stained blue (Dapi).

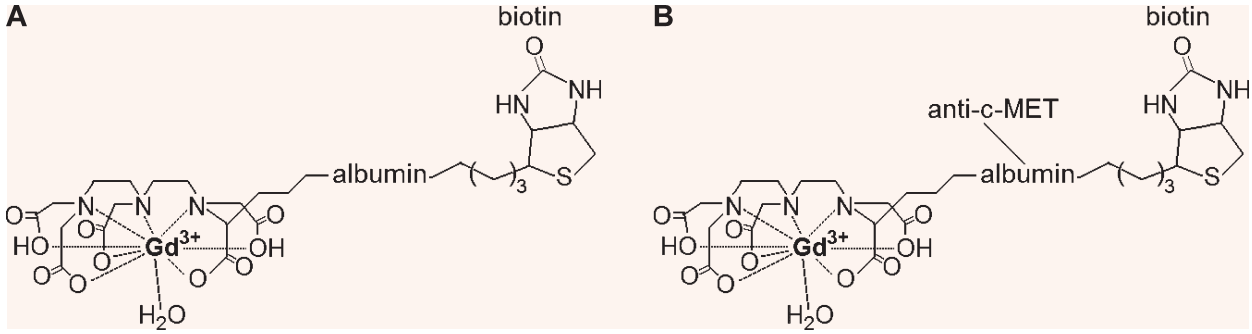

Fig. 2 Biotinyl-BSA-Gd-DTPA-based molecular targeting agent. Anti-c-Met Ab was conjugated to the albumin *via* a sulfo-link (**B**). A similar procedure was used for a normal rat IgG probe used as a control, in addition to the (**A**) non-Ab control (biotinyl-BSA-Gd-DTPA without Ab). Diagram for biotinyl-BSA-Gd-DTPA modified from ref. 39.

with horseradish peroxidase. The enhanced chemiluminescent (ECL) Advance Western Blotting Detection Kit (Amersham Biosciences, Piscataway, NJ, USA) was used to detect immunoreactive proteins.

Statistical analysis

A Student's two-tailed t-test was done between treatment groups, and brain tissue regions of interest in normal (N) and tumour periphery (TP) and interior (TI) regions. A *P*-value <0.01 or <0.05, measured between regions of interest (ROIs) or treatment groups, was considered statistically significant. Data is represented as means ± standard deviations.

Results

The C6 tumour model has been characterized in our laboratory regarding tumour volumes, tumour growth rates and expected mortality. The tumour doubling time for this glioma model is on average 2.6 days [38]. Mortality due to the glioma occurs between 17–26 days (average of 23 ± 3 days) following intracerebral implantation of C6 glioma cells [38].

Prior to molecular-targeted experiments, we initially established whether c-Met was overexpressed in the C6 glioma model. Fig. 1A shows a Western blot for c-Met protein levels between normal (contralateral control side of the brain) and glioma tissues. Fig. 1B depicts the immunofluorescence detection of c-Met in glioma tissue, compared to normal brain tissue.

In order to detect c-Met overexpression in the gliomas, we used a Gd-DTPA-albumin-based molecular targeting agent (illustration in Fig. 2), of which the Gd-DTPA-albumin moiety was previously used as a vascular MR contrast agent [35, 40]. Representative results using an albumin Gd-DTPA-based anti-c-Met molecular targeting agent in a C6 rat glioma model are shown in Fig. 3. Figure 3 (A–C) depicts a series of T_1w MR images taken pre-target agent administration (A) and a few post-contrast images taken at (B) 25 min. and (C) 3 hrs following intravenous (tail vein) administration of the Gd-DTPA-albumin-anti-c-Met targeting agent. As can be seen, there was an uptake of the targeting agent over 3 hrs. More long-term evaluation indicated that the anti-c-Met targeting agent persisted in gliomas for at least 24 hrs, and the MR signal intensity started to return to normal after 48 hrs (data not shown). Figure 3E is a histological image obtained from the normal brain tissue, as outlined in Fig. 3B. Figure 3G is a histological slide obtained from the tumour border, as illustrated in Fig. 3C. Figure 3H is a histological image obtained within a tumour necrotic centre, as outlined in Fig. 3C. Figures 3F and 3I depict the fluorescence staining for the biotinylated Gd-DTPA-albumin-anti-c-Met targeting agent (3 hrs after administration and following *in vivo* MRI investigations and excision of normal and glioma tissues) with a Cy3-streptavidin that binds the biotin located on the molecular targeting agent in the glioma (I) *versus* the normal side of the brain (F). The Gd-albumin-anti-c-Met targeting agent was clearly bound to regions of the C6 glioma, whereas the normal contralateral tissue had low-immunofluorescence staining for the targeting agent.

T_1- and T_2-weighted MR images following administration of the anti-c-Met probe (Fig. 4A and B) and

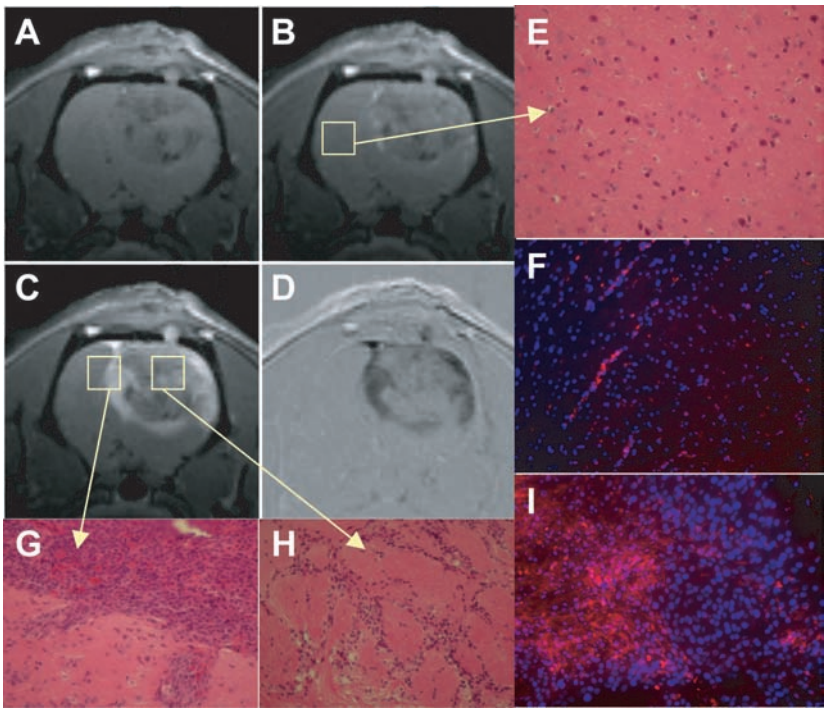

Fig. 3 T_1-weighted MR images pre- (**A**) and post-administration (**B**) 25 and (**C**) 175 min.) of anti-c-Met molecular targeting agent in a C6 glioma (23 days after implantation). (**D**) Intensity difference image between (**A**) and (**C**). Histological slices were taken from the same rat that was imaged in Figures 3A–D within normal brain tissue (**E**), a tumour border region (G; displayed rotated by 90°), and within a tumour necrotic centre (**H**). Fluorescence staining (Cy3-labelled streptavidin) of the biotin moiety of the anti-c-Met targeting agent (red fluorescence) is shown in corresponding histological slices (tumour side, I, which is the same region as histological slice H; and control brain tissue, F, which is the same region as histological slice E; 20x magnification). Nuclei are stained with Dapi (blue fluorescence). Note specific binding of the anti-c-Met probe in glioma tissue shown in frame I.

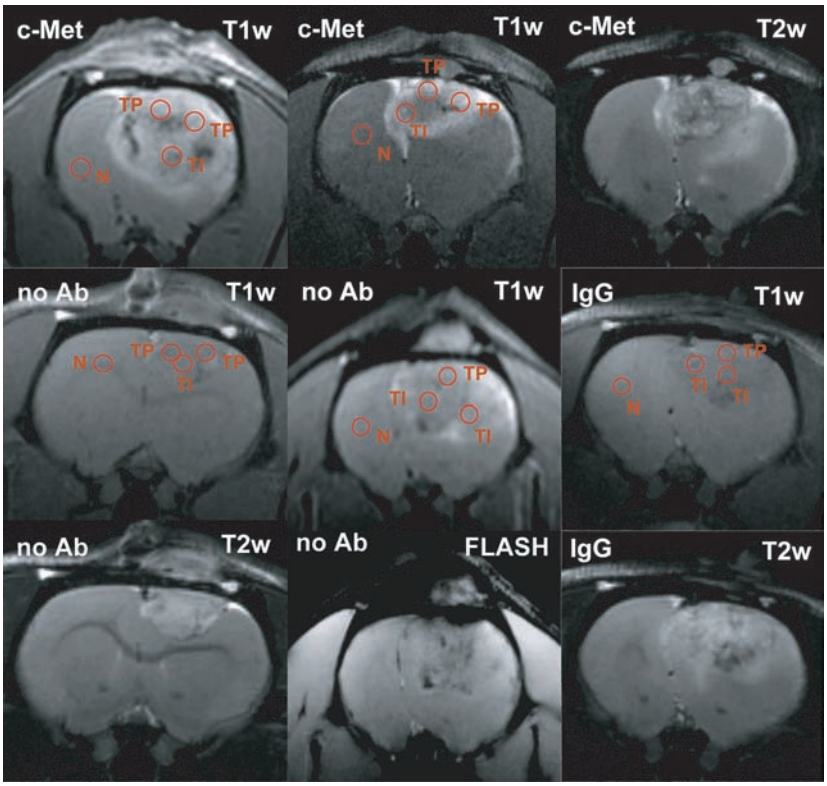

Fig. 4 T_1-weighted MR images (T1w) obtained at 3 hrs after administration of the anti-c-Met molecular targeting agent (c-Met) in rat C6 gliomas (at 23 and 17 days, respectively). Similar images have also been acquired at 3 hrs after administration of control non-Ab-Gd-DTPA-BSA (no Ab) in C6 gliomas (21 days after implantation), and control normal rat IgG-Gd-DTPA-BSA (IgG; 21 days after implantation) in C6 glioma-bearing rats. T_2-weighted images (T2w) (with the exception of the central image in the bottom panel (no Ab; FLASH), which is a FLASH image) are displayed to help depict the gliomas, since they depict a stronger contrast between the tumour and the surrounding healthy tissue in comparison to T_1-weighted images. Regions of interest used for signal intensity (SI) and T_1 measurements in Figure 5, are displayed as red circles and labelled N for normal tissue, TI for tumour interior and TP for tumour periphery regions.

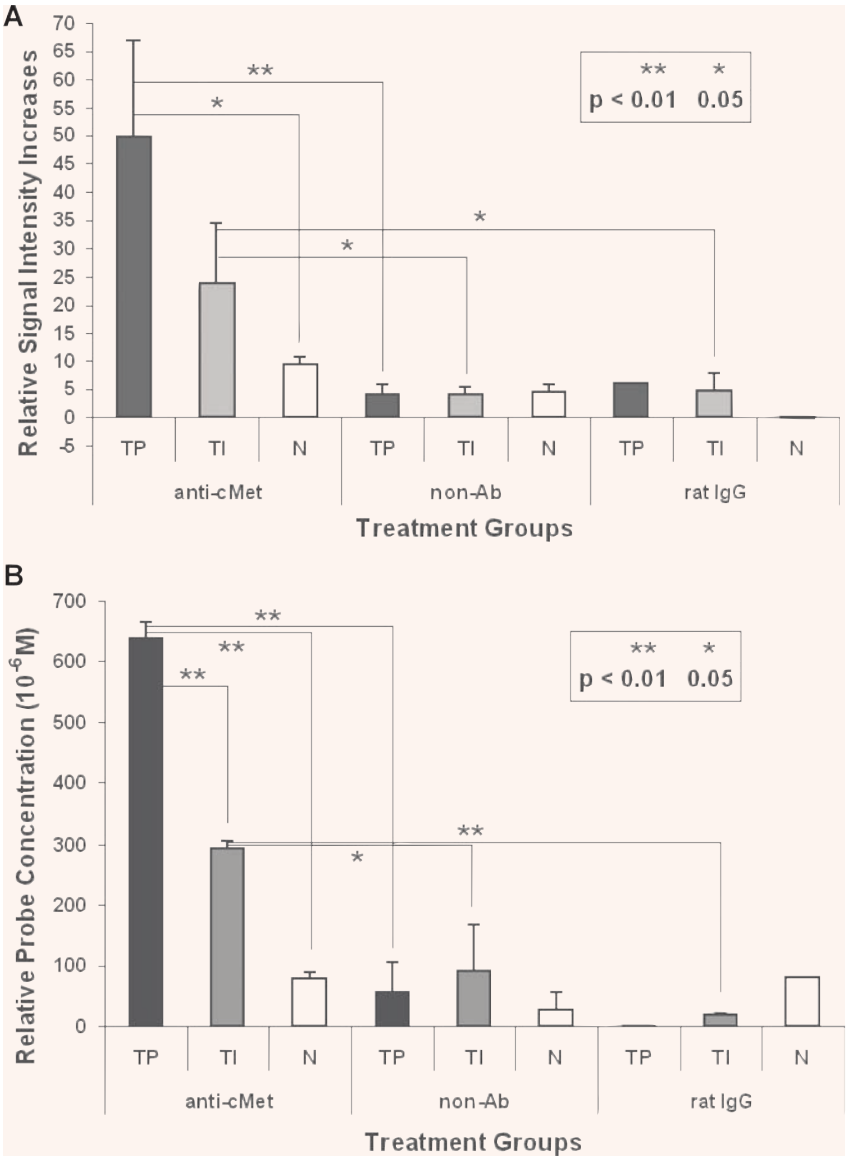

Fig. 5 Relative differences in regional (**A**) MR signal intensities and (**B**) relative probe concentrations (differences in relaxation rates [$1/T_1$] [10^{-6}M]), as outlined in each T_1-weighted image in Figure 4, following pre- and post-administration after 3 hrs, of the anti-c-Met molecular targeting agent (anti-c-Met) (region-of-interests [ROIs] shown in T1w c-Met images; in rat C6 gliomas at 23, and 17 days, respectively); pre- and post-administration, after 3 hrs, of non-Ab Gd-DTPA-BSA (non-Ab) in C6 gliomas at 21 days (from ROIs depicted in T1w no Ab images), and pre- and post-administration, after 3 hrs, of normal rat IgG-Gd-DTPA-BSA (rat IgG) in a C6 glioma at 21 days (from ROIs shown in T1w IgG images). Mean ± S.D. values for normal brain (N), tumour interior (TI) and tumour periphery (TP) are displayed in histograms. Significant differences were obtained if *P*-values were (*) <0.05, or (**) <0.01, between groups highlighted. For the normal rat IgG probe the number of regions sampled for TP and N was n = 1, that is no statistical data was obtained.

relevant controls (no Ab [Fig. 4C and D] or normal rat IgG [Fig. 4E]) are shown in Fig. 4. T_2-weighted images provided anatomical detail on tumour location, and T_1-weighted images (3 hrs following probe administration) provided MR signal information on the presence of the Gd-based probe in glioma *versus* normal brain tissues.

Regional measurements of relative differences (difference between pre- and 3 hr after administration of relevant probes) for T_1 values and MR signal intensities from ROIs (depicted in Fig. 4) obtained from T_1 maps at 3 hrs post-contrast are shown in Figure 5. ROIs were picked from T_1 maps based on high signal intensities. Previous MRI studies at 4.7 T have found that T_1 values are 1024–1035 ms for normal rat brain (non-contrast) [41] and between 1217 ms (F98 rat glioma model) [41] and 1320 ms (9L rat glioma model) [42]. For this study at 7 T, where an increase in T_1 as a function of field strength is well known [42], the pre-contrast T_1 values in the normal brain and glioma regions were 1353–1375 ms and 1309 (tumour edge regions)-1430 (tumour interior regions) ms, respectively. In the tumour regions, there was a substantial decrease in T_1 values and corresponding increases in MR signal intensities following administration of the anti-c-Met targeting

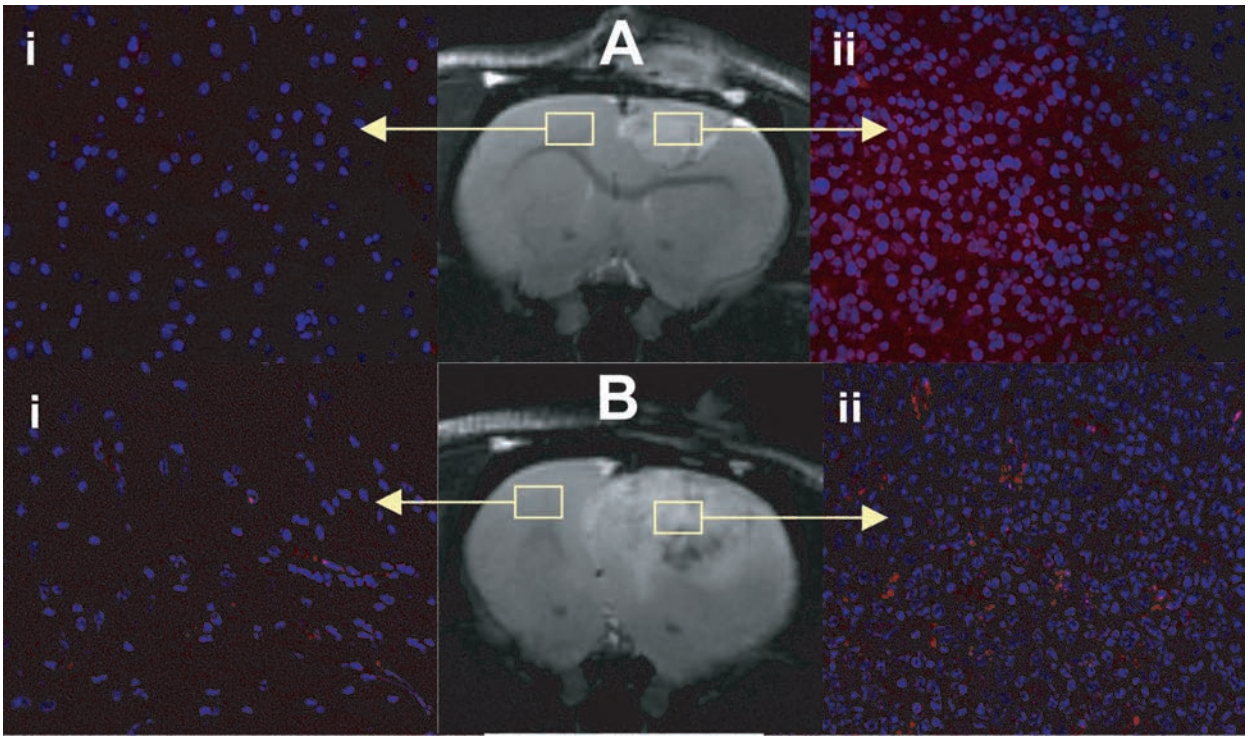

Fig. 6 T_2-weighted MR images of rats with gliomas administered with either (**A**) albumin-Gd-DTPA-biotin, or (**B**) normal rat IgG-albumin-Gd-DTPA-biotin. Outlined regions depict areas where fluorescence images were obtained following *in vivo* administration of probes. These control probes depict a lack of non-specific binding in normal (**i**) and glioma (**ii**) tissues that have undergone fluorescent staining (Cy3-labelled streptavidin) for the biotin moiety on each probe. Fluorescence staining of the biotin group on albumin-Gd-DTPA (non-specific, non-Ab) and the normal rat IgG (non-specific) probes in C6-treated rats with gliomas (Aii and Bii, respectively), and their respective normal brain tissues (Ai and Bi) on the contralateral side (magnification 20x). For a comparison see Fig. 3I, which shows specificity of the anti-c-Met probe in glioma tissue.

agent, compared to normal brain. A repetition of this experiment is shown in Figure 4B with similar increases in MR signal intensities and corresponding decreases in T_1 values within glioma regions, when compared to normal brain tissue regions (Fig. 5). Fluorescence detection of the anti-c-Met targeting agent in the gliomas depicted in Figure 4B was similar to results shown in Figure 3F and I for control brain tissue and gliomas, respectively. Control data for a non-Ab albumin-Gd-DTPA contrast agent (Fig. 4C and D), and a normal rat IgG-Gd-DTPA probe (Fig. 4E), are also shown in Figure 5. For the controls, there were minimal increases in MR signal intensity and related minimal changes in T_1 values in the glioma regions. There was also very little differentiation in the MR signal intensity or T_1 values between glioma and 'normal' brain tissues.

The absence of non-specific binding of the contrast agent was also assessed (Fig. 6). No non-specific binding of the albumin-Gd-DTPA contrast agent alone in either the glioma or normal brain tissue was detected, and a targeting agent with a normal rat IgG as the Ab moiety, also did not bind with much specificity to glioma or normal brain tissue, as compared to the anti-c-Met molecular targeting agent. For comparison, fluorescence staining for the biotin component of the anti-c-Met targeting agent only showed specificity of the probe in the glioma (Fig. 3I). Fluorescent staining was done 3 hrs following *in vivo* administration of relevant specific- and non-specific probes, MRI investigations, and subsequent removal of glioma and normal brain tissues.

Figure 7 depicts the T_1 values in rat gliomas that have been administered the anti-c-Met targeting

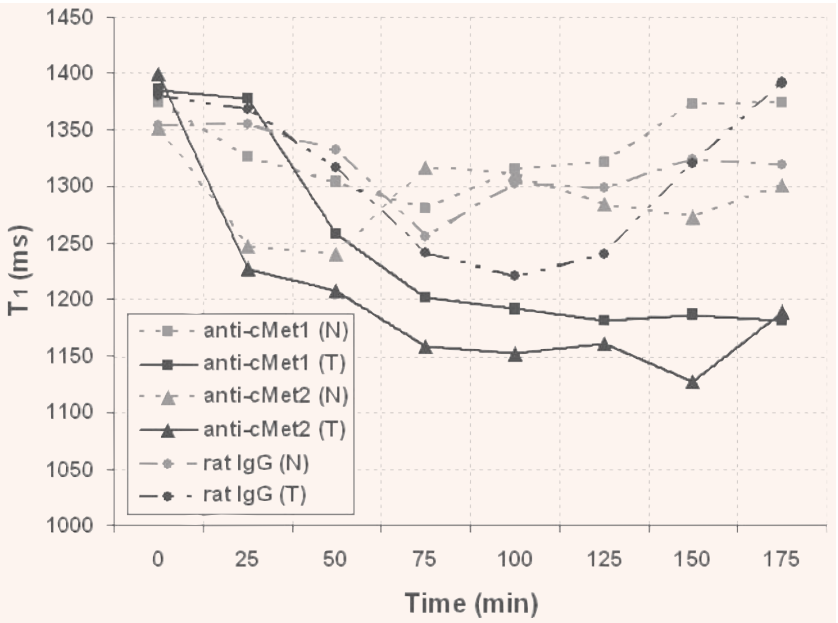

Fig. 7 T1 values in glioma and normal brain tissue from representative rats administered anti-c-Met-biotinyl-albumin-Gd-DTPA (anti-c-Met1 and anti-c-Met2), or normal rat IgG-biotinyl-albumin-Gd-DTPA, in normal (N) and tumour (T) tissues. Note a decrease in T1 values over a period of 3 hrs in glioma (T) regions of C6 rats administered the anti-c-Met targeting agent, whereas T1 values for normal brain regions return to pre-contrast T1 values after 3 hrs post-contrast.

agent (replicates, anti-c-Met1 and anti-c-Met2), in both the glioma (most central ROIs shown in Fig. 4) and 'normal' brain tissue regions. The specific ant-c-Met targeting agent remained in the gliomas after 3 hrs, whereas in 'normal' brain tissue T_1 values regress back to pre-contrast values. Likewise, the non-specific IgG Gd-DTPA-albumin contrast agent T_1 values in the tumour and 'normal' brain decrease in the first hour post-contrast agent administration, but regress back to pre-contrast T_1 values at 3 hrs post-contrast agent administration. The non-Ab Gd-DTPA-albumin contrast agent had similar results to the IgG Gd-DTPA-albumin agent (results not shown).

Depicted in Fig. 8 are probe concentration maps, derived from T_1 maps, 3 hrs following administration of either the anti-c-Met probe (Fig. 8A), the no Ab control (Fig. 8B), and the normal rat IgG control (Fig. 8C). A noticeable change in the apparent probe concentration was only observed for the anti-c-Met probe treated rat gliomas (Fig. 8A), when compared to normal brain tissue and controls in glioma tissue.

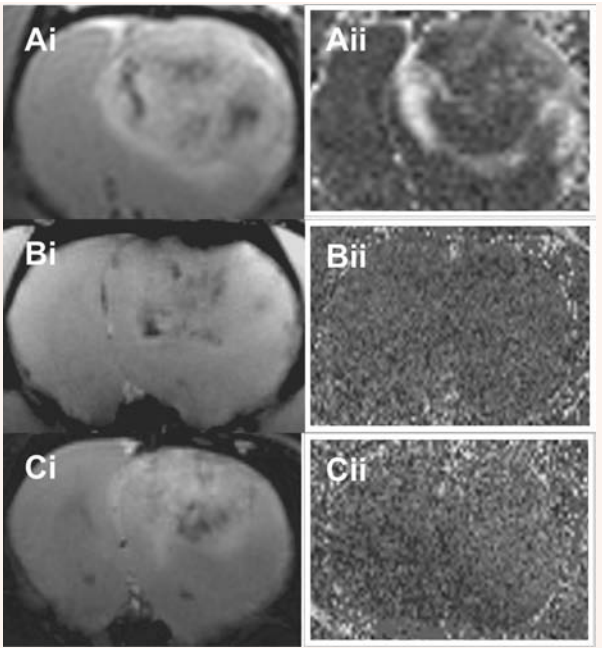

Fig. 8 (**i**) Morphological images of rats with C6 gliomas treated with (**A**) the anti-c-Met probe (T1w image, 3 hrs after anti-c-Met probe), (**B**) the non-Ab non-specific control biotinyl-albumin-Gd-DTPA contrast agent (FLASH image) and (**C**) the non-specific control normal rat IgG probe (T2w image). (**ii**) Apparent probe/contrast agent concentration maps derived from T_1 maps at 3 hrs after probe/contrast agent administration (subtracted from the pre-contrast T_1 map), for the same treatment groups as in (**i**).

Discussion

Morphological MRI was used to detect the location and size of the C6 gliomas. Tumour volumes (calculated from tumour area measurements of multiple

MRI slices using NIH ImageJ) range from 150–320 mm^3 at 17–21 days following intracerebral implantation of C6 rat glioma cells (n = 5) [38, 43]. Morphological MRI provided the necessary time-points for establishing when to administer the anti-c-Met targeting agent to visualize overexpression of c-Met in late-stage gliomas.

The multi-functional growth factor scatter factor/hepatocyte growth factor (SF/HGF) and its tyrosine kinase receptor, c-Met, have been implicated in the genesis and malignant progression of multiple human malignancies. SF/HGF is a multi-functional growth factor and its receptor, c-Met, both play a critical role in the regulation of cell growth motility, morphogenesis and angiogenesis [15, 17, 20, 21], and has been implicated in the malignant progression of gliomas [16, 17, 20]. Activation of tumour endothelial c-Met also induces extracellular matrix degradation, tubule formation and angiogenesis *in vivo* [21]. Activation of c-Met also leads to inhibition of apoptosis in tumour cells and vascular endothelial cells [21].

In intracerebrally implanted C6 rat gliomas we were able to detect higher levels of c-Met either in Western blots or fluorescence microscopic imaging (Fig. 1). The Western blots (Fig. 1A) depict c-Met for normal rat brain tissue, and a C6 glioma at 18 days after implantation of C6 glioma cells. We observed clearly higher c-Met levels in the C6 glioma tissue (Fig. 1A, right lane), when compared to the normal brain tissue (Fig. 1A, left lane), where c-Met levels were too low to be detected.

We have recently used the molecular-targeted MRI approach in being able to detect overexpression of c-Met in a rat hepatocarcinogenesis model [44]. In that model we used a super paramagnetic iron oxide (SPIO)-based anti-c-Met targeting agent to detect c-Met in hepatic nodules from a CD rat hepatocarcinogenesis model. Instead of an SPIO-based targeting agent, in the present study we decided to use a Gd-DTPA-albumin-based molecular targeting agent, which was previously used as a vascular MR contrast agent [35, 40]. It is the vascular nature of the gliomas at later stages of development that we wanted to take advantage of in order to maximize delivery of the molecular-targeted probe.

The anti-c-Met Ab was coupled to the albumin moiety of the targeting agent. In addition, a biotin tag was included for subsequent fluorescence labelling and microscopic evaluation. Gd-DTPA-albumin has been previously used as a vascular contrast agent in various tumour models to assess neovascularization [45, 46]. A biotinylated version of Gd-DTPA-albumin was also used to characterize neovasculature associated with ectopic ovarian xenotransplantation within rats [47] and lymphoangiogenesis associated with orthotopic implantation of MCF-7 human breast cancer cells in severe combined immunodeficiency (SCID) mice [48].

We used molecular-targeted imaging to visualize *in vivo* c-Met expression in C6 rat gliomas (shown in Figs 3 and 4). The Gd-based anti-c-Met-targeting agent was found to specifically bind to C6 glioma tissue, as shown by the relative probe concentration maps (Fig. 8), a decrease in T_1 relaxation values (Fig. 6), increased relative probe concentrations in Figure 5, and an increase in MR signal intensities (see Fig. 5). We observed an uptake of the targeting agent over time, which stabilized over the 3 hrs time-point. The Gd-based anti-c-Met targeting agent was found to specifically bind to regions of the C6 glioma, as determined by immunofluorescence labelling of the biotin moiety of the anti-c-Met biotinyl-albumin-Gd-DTPA targeting agent (see Fig. 3) administered intravenously to rats with late stage gliomas (17–21 days following intracerebral implantation of C6 rat glioma cells, that is when tumours occupy >25% of the affected cerebral cortex). Histological slices were obtained from the same rat that molecular-targeted MRI was obtained from in Fig. 3, using MRI spatial co-ordinates. Repeated samples indicated a similar response (histological fluorescence data not shown), in comparison to normal brain tissue regions or control samples administered the contrast agent (albumin-Gd-DTPA) alone or with normal rat IgG of similar molecular weight to the anti-c-Met molecular targeting complex (see Fig. 5).

Figure 6 further supports the specific binding of the anti-c-Met targeting agent to gliomas only, as the T_1 values remain decreased 3 hrs after administration of the targeting agent. Non-specific distribution of the anti-c-Met targeting agent in 'normal' brain tissue and non-specific distribution of the non-Ab labelled Gd-DTPA-albumin complex in both tumour and normal brain regions was clearly illustrated. It is also noteworthy that most of the anti-c-Met targeting agent was mainly distributed in the outer regions of the glioma, which may reflect the vascular nature of the tumour, and seem to be concentrated in the outer periphery regions of the tumour [38].

This distribution of the anti-c-Met targeting agent is further substantiated by the relative probe concentration

maps generated from T_1 maps. These relative concentration maps indicate that there was specific uptake of the anti-c-Met probe in peripheral glioma regions depicted in Fig. 8A, and no detected selective uptake in normal tissues. The significant increases of the relative concentration of the anti-c-Met probe in the tumours, particularly the peripheral regions, is due to the vascular nature of the gliomas and that the Gd-DTPA-albumin contrast agent framework is a blood-pool agent. The Gd-DTPA-albumin contrast-based probe is readily eliminated from tissue if it does not bind to specific receptors. The decreased levels of the anti-c-Met probe in the tumour interior may be due to the limited vascularity of the tumour in these regions. Relative concentrations of the no-Ab and normal rat IgG non-specific probes/contrast agents were low to non-detectable in either glioma or normal tissues at 3 hrs after administration.

The fluorescence labelling of the anti-c-Met targeting agent in the normal brain tissue did indicate some signal from the brain vasculature, which may be due to re-circulation of the targeting agent and/or shedding of c-Met into blood. It has already been established that c-Met expression is normally found to be low in the non-challenged vascular endothelium [23], eliminating the vascular endothelium as a source of c-Met that was detected in the vasculature by immunofluorescence tagging of the anti-c-Met targeting agent. Another possible explanation can be surmised from a report of the detection of soluble c-Met detected in plasma samples from mice that received UOK261 (human bladder carcinoma cells) xenografts [49]. Athauda *et al.* hypothesized that the increased plasma levels of c-Met were due to ectodomain shedding of c-Met which was overexpressed in cancer [49]. They also found that the shedding rate correlated with malignant potential [49]. The uptake of the probes/contrast agents (both specific for c-Met and non-specific controls) in normal tissue was unusual as no damage to the blood-brain-barrier (BBB) was expected, however there still was some uptake of the probes in blood vessels as illustrated in Fig. 3F.

The results from this study clearly illustrate that the anti-c-Met Gd-DTPA-albumin-based targeting agent is specific for the detection of c-Met in gliomas *in vivo* with MRI. A practical application of this method would be to predict the malignant potential of a tumour.

Acknowledgements

We would like to thank Mr. Rajibul Alam for assistance in image data analysis for signal intensities. The research was supported by the National Institutes of Health (NIH 5R03CA121359-2 grant) and the Oklahoma Center for the Advancement of Sciences and Technology (OCAST OARS AR052-132 grant).

References

1. **Sanson M, Thillet J, Hoang-Xuan K.** Molecular changes in gliomas. *Curr Opin Oncol.* 2004; 16: 607–13.
2. **Legler JM, Ries LA, Smith MA, Warren JL, Heineman EF, Kaplan RS, Linet MS.** Cancer surveillance series: brain and other central nervous system cancers: recent trends in incidence and mortality. *J Natl Cancer Inst.* 1999; 91: 1382–90.
3. **Kish PE, Blaivas M, Strawderman M, Muraszko KM, Ross DA, Ross BD, McMahon G.** MRI of ethylnitrosourea-induced rat gliomas: a model for experimental therapeutics of low-grade gliomas. *J Neuro-Oncology.* 2001; 53: 243–57.
4. CBTRUS 2002: Statistical Report: Primary Brain Tumors in the United States. 1995-1999: Central Brain Tumor Registry of the United States, 2002.
5. **Demuth T, Berens ME.** Molecular mechanisms of glioma cell migration and invasion. *J Neuro-Oncol.* 2004; 70: 217–28.
6. **Rao RD, James CD.** Altered molecular pathways in gliomas: an overview of clinically relevant issues. *Semin Oncol.* 2004; 31: 595–604.
7. **Kobayashi N, Allen N, Clendenon NR, Ko LW.** An improved rat brain-tumor model. *J Neorosurg* 1980; 53: 808–15.
8. **Berstein JJ, Goldberg WJ, Laws Jr ER, Conger D, Morreale V, Wood LR.** C6 glioma cell invasion and migration of rat brain after neural homografting: untrastructure. *Neurosurgery.* 1990; 26: 622–8.
9. **Saini M, Bellinzona M, Meyer F, Cali G, Samii M.** Morphometrical characterization of two glioma models in the brain of immunocompetent and immunodeficient rats. *J Neurooncol.* 1999; 42: 59–67.
10. **Grobben B, De Deyn PP, Slegers H.** Rat C6 glioma as experimental model system for the study of glioblastoma growth and invasion. *Cell Tissue Res.* 2002; 310: 257–70.
11. **Zhang X, Wu J, Gao D, Fei Z, Qu Y, Jing J.** Development of a rat C6 brain tumor model. *Chin Med J.* 2002; 115: 455–7.
12. **Elias MC, Tozer KR, Silber JR, Mikheeva S, Deng M, Morrison RS, Manning TC, Silbergeld DL,**

Glackin CA, Reh TA. Rostomily RC. TWIST is expressed in human gliomas and promotes invasion. *Neoplasia.* 2005; 7: 824–37.

13. **Ziegler A, von Kienlin M, Decorps M, Remy C.** High glycolytic activity in rat glioma demonstrated *in vivo* by correlation peak ^{1}H magnetic resonance imaging. *Cancer Res.* 2001; 61: 5595–600.
14. **Zeng Z, Weiser MR, D'Alessio M, Grace A, Shia J, Paty PB.** Immunoblot analysis of c-Met expression in human colorectal cancer: overexpression is associated with advanced stage cancer. *Clin*. Exp. *Metastasis.* 2004; 21: 409–17.
15. **DiRenzo MF, Narshimhan RP, Olivero M, Bretti S, Giordano S, Medico E, Gaglia P, Zara P, Comoglio PM.** Expression of the Met/HGF receptor in normal and neoplastic tissues. *Oncogene.* 1991; 6: 1997–2003.
16. **Koochekpour S, Jeffers M, Rulong S, Taylor G, Klineberg E, Hudson EA, Resau JH, Vande Woude GF.** Met and hepatocyte growth factor/scatter factor expression in human gliomas. *Cancer Res.* 1997; 57: 5391–8.
17. **Lamszus K, Liang J, Laterra J, Zagzag D, Way D, Witte M, Goldberg ID, Rosen EM.** Scatter factor promotes motility of human glioma and neuromicrovascular endothelial cells. *In J Cancer.* 1998; 75: 19–28.
18. **Moriyama T, Kataoka H, Kawano Y, Yokogami K, Nakano S, Goya T, Uchino H, Koono M, Wakasaka S.** Comparative analysis of expression of hepatocyte growth factor and its receptor, c-met, in gliomas, meningiomas and schwannomas. *Cancer Lett.* 1998; 124: 149–55.
19. **Yu Y, Merlino G.** Constitutive c-MET signaling through a nonautocrine mechanism promotes metastasis in a transgenic transplantation model. *Cancer Res.* 2002; 62: 2951–6.
20. **Arrieta O, Garcia E, Guevara P, Garcia-Navarrete R, Ondarza R, Rembao D, Sotelo J.** Hepatocyte growth factor is associated with poor prognosis of malignant gliomas and is a predictor for recurrence of *meningioma. Cancer.* 2002; 94: 3210–8.
21. **Abounader R, Laterra J.** Scatter factor/hepatocyte growth factor in brain growth and angiogenesis. *Neuro-oncol.* 2005; 7: 436–51.
22. **Abounader R, Ranganathan S, Lal B, Fielding K, Book A, Dietz H, Burger P, Laterra J.** Reversion of human glioblastoma malignancy by U1 small nuclear RNA/ribozyme targeting of scatter factor/hepatocyte growth factor and c-Met expression. *J Natl Cancer Inst.* 1999; 91: 1548–56.
23. **Yuan R, Durden DL, Van Meir EG, Brat DJ.** Pseudopalisading necrosis in glioblastoma: a familiar morphologic feature that links vascular pathology, hypoxia, and angiogenesis. *J Neuropathol. Exp. Neurol.* 2006; 65: 529–39.
24. **Li KCP, Bednarski MD.** Vascular-targeted molecular imaging using functionalized polymerized vesicles. *J Magn Reson Imaging.* 2002; 16: 388–93.
25. **Sipkins DA, Cheresh DA, Kazemi MR, Nevin LM, Berdnarski MD, Li KCP.** Detection of tumor angiogenesis *in vivo* by $\alpha_V\beta_3$-targeted magnetic resonance imaging. *Nat Med.* 1998; 4: 623–6.
26. **Sipkins DA, Gijbels K, Tropper FD, Bednarski M, Li KC, Steinman L.** ICAM-1 expression in autoimmune encephalitis visualized using magnetic resonance imaging. *J Neuroimmunol.* 2000; 104: 1–9.
27. **Konda SD, Aref M, Wang S, Brechbiel M, Wiener EC.** Specific targeting of folate-dendrimer MRI contrast agents to the high affinity folate receptor expressed in ovarian tumor xenografts. Magn. Reson. *Materials Physics Biol. Med.* 2001; 12: 104–13.
28. **Artemov D, Mori N, Ravi R, Bhujwalla ZM.** Magnetic resonance molecular imaging of the HER-2/neu receptor. *Cancer Res.* 2003; 63: 2723–7.
29. **Schmidt KF, Ziu M, Schmidt NO, Vaghasia P, Cargioloi TG, Doshi S, Albert MS, Black PMcL, Carroll RS, Sun Y.** Volume reconstruction techniques improve the correlation between histological and *in vivo* tumor volume measurements in mouse models of human gliomas. *JNeuro-Oncology.* 2004; 68: 207–15.
30. **Badruddoja MA, Krouwer HG, Rand SD, Rebro KJ, Pathak AP, Schmainda KM.** Antiangiogenic effects of dexamethasone in 9L gliosarcoma assessed by MRI cerebral blood volume maps. *Neuro-Oncol.* 2003; 5: 235–43.
31. **Pathak AP, Schmainda KM, Ward BD, Linderman JR, Rebro KJ, Greene AS.** MR-derived cerebral blood volume maps: issues regarding histological validation and assessment of tumor angiogenesis. *Magn Reson Med.* 2001; 46: 735–47.
32. **Moore A, Marecos E, Bogdanov A, Weissleder R.** Tumoral distribution of long-circulating dextran-coated iron oxide nanoparticles in a rodent model. *Radiology.* 2000; 214: 568–74.
33. **Benda P, Lightbody J, Sato G, Levine L, Sweet W.** Differentiated rat glial cell strain in tissue culture. *Science.* 1968; 161: 370–1.
34. **Trusolino L, Comoglio PM.** Scatter-factor and semaphorin receptors: cell signalling for invasive growth. *Nature Reviews.* 2002; 2: 289–99.
35. **Dafni H, Landsman L, Schechter B, Kohen F, Neeman M.** MRI and fluorescence microscopy of the acute vascular response to VEGF165: vasodilation, hyper-permeability and lymphatic uptake, followed by rapid inactivation of the growth factor. *NMR in Biomedicine.* 2002; 15: 120–31.
36. **Hermanson G.** Bioconjugate Techniques. Academic Press, New York, p. 176, 1996.

37. **Haacke EM, Brown RW, Thompson MR, Venkatesan R.** Magnetic resonance imaging: physical principles and sequence design. *Wiley-Liss;* 1999
38. **Doblas S, Saunders D, Kshirsagar P, Pye Q, Oblander J, Gordon B, Kosanke S, Floyd RA. Towner RA.** Phenyl-tert-butyl-nitrone induces tumor regression and decreases angiogenesis in a C6 rat glioma model. *Free Radical Biol Med.* 2008; 44: 63–72.
39. **Dirksen A, Langereis S, de Waal BFM, van Gendersen MHP, Hackeng TM, Meijer EW.** A supramolecular approach to multivalent target-specific MRI contrast agents for angiogenesis. *Chem Commun.* 2005; 14: 2811–3.
40. **Ogan MD, Schmiedl U, Moseley ME, Grodd W, Paajanen H, Brasch RC.** Albumin labelled with Gd-DTPA. An intravascular contrast-enhancing agent for magnetic resonance blood pool imaging: preparation and characterization. *Invest Radiol.* 1987; 22: 665–71.
41. **Hoehn-Berlage M, Norris D, Bockhorst K, Ernestus R-I, Kloiber O, Bonnekoh P, Leibfritz D, Hossmann K-A.** T1 Snapshot FLASH measurement of rat brain glioma: kinetics of the tumor-enhancing contrast agent manganese (III) tetraphenylporphine sulfonate. *Magn Reson Med.* 1992; 27: 201–13.
42. **Rajan SS, Rosa L, Francisco J, Muraki A, Carvlin M, Tuturea E.** MRI characterization of 9L-glioma in rat brain at 4.7 Tesla. *Magn Reson Imaging.* 1990; 8: 185–90.
43. **Doblas S, Tesiram Y, Saunders D, Pye Q, Kshirsagar P, Towner RA.** Characterization of rat glioma models by magnetic resonance angiography. Proceedings of 14th Annual Meeting of ISMRM, Abs. 1745, 2006.
44. **Towner RA, Smith N, Tesiram YA, Abbott A, Saunders D, Blindauer R, Herlea O, Silasi-Mansat R, Lupu F.** *In vivo* detection of c-Met expression in a rat hepatocarcinogenesis model using molecularly targeted magnetic resonance imaging. *Molecular Imaging.* 2007; 6: 18–29.
45. **Marzola P, Degrassi A, Calderan L, Farace P, Crescimanno C, Nicolato E, Giusti A, Pesenti E, Terron A, Sbarbati A, Abrams T, Murray L, Osculati F.** *In vivo* assessment of antiangiogenic activity of SU6668 in an experimental colon carcinoma model. *Clin Can Res.* 2004; 10: 739–50.
46. **Bhujwalla ZM, Artemov D, Natarajan K, Ackerstaff E, Solaiyappan M.** Vascular differences detected by MRI for metastatic *versus* nonmetastatic breast and prostate cancer xenografts. *Neoplasia.* 2001; 3: 143–53.
47. **Israely T, Dafni H, Nevo N, Tsafriri A, Neeman M.** Angiogenesis in ectopic ovarian xenotransplantation: multiparameter characterization of the neovasculature by dynamic contrast-enhanced MRI. *Magn Reson Med.* 2004; 52: 741–50.
48. **Pathak AP, Artemov D, Ward BD, Jackson DG, Neeman M, Bhujwalla ZM.** Characterizing extravascular fluid transport of macromolecules in the tumor interstitium by magnetic resonance imaging. *Cancer Res.* 2005; 65: 1425–32.
49. **Athauda G, Giubellino A, Coleman JA, Horak C, Steeg PS, Lee M-JJ, Trepel J, Wimberly J, Sun J, Coxon A, Burgess TL, Bottaro DP.** c-Met ectodomain shedding rate correlates with malignant potential. *Clin Cancer Res.* 2006; 12: 4154–62.